Stratospheric Control of the Madden–Julian Oscillation

SEOK-WOO SON AND YUNA LIM

School of Earth and Environmental Sciences, Seoul National University, Seoul, South Korea

CHANGHYUN YOO

Department of Atmospheric Sciences and Engineering, Ewha Womans University, Seoul, South Korea

HARRY H. HENDON

Bureau of Meteorology, Melbourne, Victoria, Australia

JOOWAN KIM

Department of Atmospheric Sciences, Kongju National University, Kongju, South Korea

(Manuscript received 21 August 2016, in final form 14 November 2016)

ABSTRACT

Interannual variation of seasonal-mean tropical convection over the Indo-Pacific region is primarily controlled by El Niño–Southern Oscillation (ENSO). For example, during El Niño winters, seasonal-mean convection around the Maritime Continent becomes weaker than normal, while that over the central to eastern Pacific is strengthened. Similarly, subseasonal convective activity, which is associated with the Madden–Julian oscillation (MJO), is influenced by ENSO. The MJO activity tends to extend farther eastward to the date line during El Niño winters and contract toward the western Pacific during La Niña winters. However, the overall level of MJO activity across the Maritime Continent does not change much in response to the ENSO. It is shown that the boreal winter MJO amplitude is closely linked with the stratospheric quasi-biennial oscillation (QBO) rather than with ENSO. The MJO activity around the Maritime Continent becomes stronger and more organized during the easterly QBO winters. The QBO-related MJO change explains up to 40% of interannual variation of the boreal winter MJO amplitude. This result suggests that variability of the MJO and the related tropical–extratropical teleconnections can be better understood and predicted by taking not only the tropospheric circulation but also the stratospheric mean state into account. The seasonality of the QBO–MJO link and the possible mechanism are also discussed.

1. Introduction

Large-scale tropical convection plays a crucial role in modulating not only the tropical hydrology and climate but also extratropical weather and climate through its teleconnections. For instance, subseasonal and seasonal variations of organized convection over the equatorial western Pacific often excite Rossby waves that propagate from the subtropical North Pacific to Alaska and then to Florida, affecting precipitation and surface air temperature across the North Pacific and North America (Wallace and Gutzler 1981; Jin and Hoskins 1995; Seo and Son 2012). Such a teleconnection is especially well defined during boreal winter [December–February (DJF)], allowing extended weather and climate predictions in the extratropics (Robertson et al. 2015).

Tropical convection, especially around the Maritime Continent, is not static but varies significantly in time and space. On interannual time scale, seasonal-mean convection is largely modulated by El Niño–Southern Oscillation (ENSO), which is the leading mode of interannual variability in the tropical troposphere and ocean. For example, during La Niña winters, seasonal-mean tropical convection over the Maritime Continent is strengthened, while that over the central and eastern

Corresponding author e-mail: Seok-Woo Son, seokwooson@snu.ac.kr

DOI: 10.1175/JCLI-D-16-0620.1

Pacific is weakened. This is due to the enhanced Walker circulation in response to a strengthened east–west sea surface temperature (SST) gradient across the tropical Pacific. The opposite is true during El Niño winters. Although relatively minor and less robust, it has been documented that seasonal-mean tropical convection is also influenced by the stratospheric quasi-biennial oscillation (QBO), which is the leading mode of interannual variability in the tropical stratosphere. Both observational and modeling studies have shown the evidence of QBO-related seasonal-mean convection and precipitation changes (Giorgetta et al. 1999; Collimore et al. 2003; Garfinkel and Hartmann 2011; Liess and Geller 2012), with an enhanced deep convection over the western Pacific during boreal winter in the easterly phase of the QBO (Collimore et al. 2003; Liess and Geller 2012).

ENSO and the QBO regulate not only seasonal-mean tropical convection but also subseasonal convective activity, such as the Madden–Julian oscillation (MJO; Madden and Julian 1994), during boreal winter (e.g., Pang et al. 2016; Yoo and Son 2016). Both the spatial structure and amplitude of the MJO vary from year to year in response to ENSO and the QBO. These changes can then modify the tropical–extratropical teleconnections. However, unlike the ENSO, the impacts of the QBO on MJO activity and the related teleconnections have not been well documented until very recently (Liu et al. 2014; Yoo and Son 2016; Marshall et al. 2016; Nishimoto and Yoden 2017).

The present study demonstrates that while the spatial pattern of the seasonal-mean convection and the MJO-related subseasonal convective activity is primarily controlled by the ENSO, the year-to-year variation of overall level of subseasonal convective activity over the central Indian Ocean to the western Pacific, including the MJO, is significantly modulated by the QBO. These different roles of the ENSO and QBO are quantified by performing composite and correlation analyses. After briefly evaluating their relative importance on the seasonal-mean convection in section 3, their impacts on the MJO-related subseasonal convective activity are analyzed in detail in section 4. Extending Yoo and Son (2016), particular attention is paid to the impact of the QBO on the MJO and the related teleconnections during boreal winter. The seasonality and possible mechanism(s) of the QBO–MJO link are also discussed.

2. Data and methods

This study is mostly based on observational data analyses. The only exception is the reanalysis data from the European Center for Medium-Range Weather Forecasts (ECMWF), that is, ERA-Interim (Dee et al. 2011), from 1979 to 2015. These data are used to define the QBO and to examine the QBO-related atmospheric circulation changes.

The QBO-related wind and temperature profile changes are examined using radiosonde observations from the Integrated Global Radiosonde Archive (IGRA; Durre et al. 2006). Only six stations around the Maritime Continent are considered. In terms of station number and geographical location, they are stations 96163 (0.88°S, 100.35°E), 96237 (2.17°S, 106.13°E), 97072 (0.68°S, 119.73°E), 97180 (5.07°S, 119.55°E), 97560 (1.18°S, 136.12°E), and 97724 (3.70°S, 128.08°E). For the easterly QBO (EQBO) and westerly QBO (WQBO) winters, a total of 2176 and 3241 soundings, respectively, are used from 1979 to 2013 (see below for the definition of EQBO and WQBO winters). The high-resolution temperature profiles and the tropopause temperature distributions are also examined by using the global positioning system (GPS) radio occultation (RO) measurements from the Constellation Observing System for Meteorology, Ionosphere and Climate (COSMIC) mission (Anthes et al. 2008) from 2006 to 2015.

Various satellite observations are also used. They include the National Oceanic and Atmospheric Administration (NOAA) Extended Reconstructed Sea Surface Temperature data (ERSST.v4; Huang et al. 2016) from 1979 to 2013, the NOAA interpolated outgoing longwave radiation (OLR) data from 1979 to 2013 (Liebmann and Smith 1996), and the Tropical Rainfall Measuring Mission (TRMM) precipitation data from 1998 to 2013 (Liu et al. 2012). The latter two datasets are used to infer variations in organized tropical convection. To examine cloud distribution near the tropopause, Cloud–Aerosol Lidar with Orthogonal Polarization (CALIOP) level-2 products (Winker et al. 2007) are also used from 2006 to 2015. Note that each dataset covers different time periods. Most analyses are performed until 2013 because NOAA OLR data are unavailable after 2014. However, for the COSMIC and CALIOP datasets, all available data are used to increase the sample size.

The COSMIC GPS RO and CALIOP measurements are not gridded datasets. To make a direct comparison with other datasets, they are gridded as follows. The vertical resolution of COSMIC data is set to 200 m (Son et al. 2011; Kim and Son 2012), and the tropopause is defined with the coldest level in each temperature profile. The resulting temperature profiles and tropopause properties are then simply averaged over 5° longitude × 5° latitude nonoverlapping grid boxes for each month. Roughly 10–30 observations per month are used for each grid box, depending on the time and latitude band (Son et al. 2011). The CALIOP products are originally provided

with a 5-km horizontal resolution. They are gridded over 10° longitude × 10° latitude grid boxes (Sassen et al. 2008). For a given grid box, the fraction of cirrus clouds, which includes both isolated thin clouds and anvil clouds, is defined by the ratio of the returns that are detected as clouds with a cloud base above 15 km.

a. ENSO index

ENSO is simply defined by the Niño-3.4 (5°S–5°N, 170°–120°W) SST anomaly. When the DJF-mean Niño-3.4 SST anomaly is greater than 0.5 standard deviation, it is set to the El Niño winter. The opposite (i.e., SST anomaly smaller than −0.5 standard deviation) is set to the La Niña winter. For the analysis period of 1979–2013, a total of 10 and 12 years are identified as El Niño and La Niña winters, respectively. Strong ENSO years, addressed in the next subsection, are also defined with plus or minus one standard deviation.

b. QBO index

The QBO is typically characterized by the downward propagation of zonal-mean zonal wind in the equatorial stratosphere (Baldwin et al. 2001). As such, several indices with varying vertical levels have been used in the literature. In this study, the QBO is defined by zonal-mean zonal wind at 50 hPa averaged over 10°S–10°N (U50) from ERA-Interim data, unless otherwise specified. When the seasonal-mean U50 is easterly and smaller than −0.5 standard deviation, it is set to the EQBO. Likewise, the opposite (i.e., westerly and greater than 0.5 standard deviation) is set to the WQBO. Note that the QBO has been often defined by using long-term rawinsonde observations in the tropics (e.g., Naujokat 1986). Although station datasets are always preferable, one or two stations may not effectively represent the QBO-related zonal-mean circulation change as they could be influenced by local circulation.

The fact that the QBO oscillates approximately every 28 months (Baldwin et al. 2001) implies that the number of EQBO and WQBO years can be different. For the analysis period of 1979–2013, a total of 10 and 15 years are identified as EQBO and WQBO winters, respectively. When strong ENSO years are excluded, they become more evenly distributed with eight EQBO and nine WQBO winters. Here it should be emphasized that although the QBO is driven by equatorial waves, which systematically break in the stratosphere, those waves are only partly (not all) excited by large-scale tropical convection. As such, the QBO is only weakly correlated with ENSO. The maximum correlation between the Niño-3.4 index and various QBO indices at different levels is only 0.21, and this value is not statistically significant.

c. MJO index

The MJO phase and amplitude are defined by the OLR-based MJO index (OMI; Kiladis et al. 2014). Unlike the real-time MJO index (Wheeler and Hendon 2004), this index is solely based on the satellite-derived OLR and more directly discriminates convective signature of the MJO. The OMI consists of the leading pair of empirical orthogonal functions of bandpass-filtered OLR over 20°S–20°N. The two leading principal components (i.e., PC1 and PC2, which are directly obtained online from the NOAA/Earth System Research Laboratory website http://www.esrl.noaa.gov/psd/mjo/mjoindex) are then used to define the MJO phase and amplitude. Following the convention of Wheeler and Hendon (2004), the MJO phase is determined in the PC1–PC2 space. Likewise, the MJO amplitude (more precisely, the OMI amplitude) is defined by the square root of the sum of the squared daily values of the two leading PCs [i.e., $(PC1^2 + PC2^2)^{1/2}$]. Although not shown, other MJO indices are also tested (Yoo and Son 2016). It turns out that overall results are not sensitive to the choice of the MJO index.

3. Interannual modulation of seasonal-mean tropical convection by the ENSO

We first examine the relative importance of the ENSO and the QBO on the seasonal-mean tropical convection (Figs. 1a–c). Figure 1a presents the climatological distribution of the DJF-mean convection in terms of OLR. Three hot spots are evident across the intertropical convergence zone. On interannual time scale, these convective centers, especially those over the western to central Pacific, undergo a significant variation in response to the ENSO (e.g., Martin et al. 2004). Between El Niño and La Niña winters, seasonal-mean OLR exhibits statistically significant differences across the Pacific. Here, statistical significance is tested with Welch's *t* test (Inoue et al. 2011). Quantitatively, ENSO-related seasonal-mean OLR change is up to 10% of the climatological OLR, with mean convection shifted eastward to the date line and weakened around the Maritime Continent during El Niño winters (cf. Figs. 1a,b). The opposite is true during La Niña winters. These changes reflect a weakened (strengthened) Walker circulation during El Niño (La Niña) winters. Not surprisingly, correlations between DJF-mean OLR, averaged across the Maritime Continent (110°–140°E), and various ENSO indices are very high and statistically significant (see the first OLR column in Table 1).

On the other hand, the QBO-related change in seasonal-mean OLR is rather minor (Fig. 1c). As reported in the previous studies, an enhanced convection

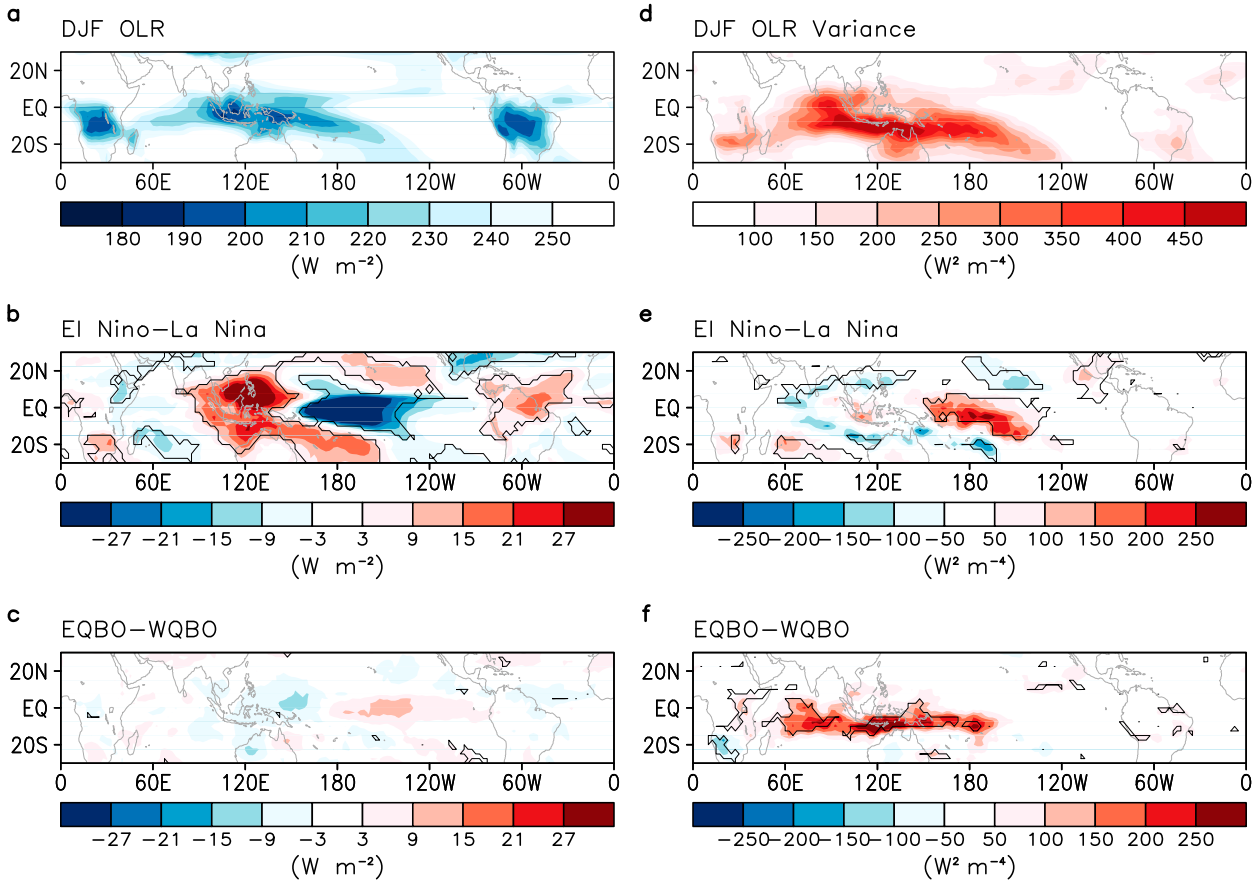

FIG. 1. DJF-mean OLR and bandpass-filtered (20–100 days) OLR variance: (a),(d) long-term climatology, (b),(e) interannual difference between El Niño and La Niña winters, and (c),(f) difference between EQBO and WQBO winters. In (b),(c),(e),(f), statistically significant values at the 95% confidence level are contoured.

over the western Pacific and a weakened convection over the eastern Pacific are observed during EQBO winters (e.g., Collimore et al. 2003; Liess and Geller 2012). However, these changes are much smaller than ENSO-related changes and not statistically significant. As such, no meaningful correlations are observed between the DJF-mean OLR, averaged across the Maritime Continent, and various QBO indices (Table 1).

The above result (i.e., regulation of the DJF-mean convection by the ENSO with a minor contribution of the QBO) is largely insensitive to the season (Table 1). In all seasons, seasonal-mean OLR anomalies around

TABLE 1. Correlations of seasonal-mean OLR, averaged across the Maritime Continent (15°S–5°N, 110°–140°E), and MJO amplitude against various ENSO and QBO indices from 1979 to 2013. Niño-3, Niño-3.4, and Niño-4 indices are used as the ENSO indices. Likewise, for the QBO indices, zonal-mean zonal wind, averaged over 10°N–10°S, at 10 hPa (U10), 20 hPa (U20), 30 hPa (U30), and 50 hPa (U50) are used. Statistically significant values at the 95% confidence levels are denoted with an asterisk.

		OLR (Maritime Continent)				MJO amplitude			
		DJF	MAM	JJA	SON	DJF	MAM	JJA	SON
ENSO	Niño-3	0.84*	0.47*	0.70*	0.83*	−0.08	−0.19	0.04	−0.14
	Niño-3.4	0.85*	0.64*	0.83*	0.86*	−0.01	0.00	0.20	−0.15
	Niño-4	0.74*	0.69*	0.79*	0.81*	0.11	0.26	0.24	−0.08
QBO	U10	0.02	0.15	0.11	−0.03	0.63*	0.20	−0.01	−0.18
	U20	−0.04	0.09	0.20	0.23	0.33	0.22	−0.17	−0.18
	U30	0.04	0.02	0.10	0.32	−0.16	0.19	−0.23	−0.03
	U50	0.18	−0.04	−0.05	0.18	−0.57*	−0.09	−0.09	0.10

the Maritime Continent–western Pacific are highly correlated with ENSO. Although correlations are relatively weak during boreal summer, they are still statistically significant. In contrast, in all seasons, no significant correlations are found for the QBO. These results confirm that the interannual variation of the seasonal-mean tropical convection is predominantly controlled by the ENSO.

4. Interannual modulation of subseasonal tropical convective activity by the QBO

On subseasonal time scale, tropical convection exhibits substantial variability. Figure 1d presents the spatial distribution of bandpass-filtered (20–100 days) OLR variance during boreal winter. Strong variability is observed mostly in the Indo-Pacific warm pool region, largely representing the MJO (Madden and Julian 1994). This localized OLR variance resembles the regional pattern of seasonal-mean convection (cf. Fig. 1a). However, there is a subtle difference over the Maritime Continent (e.g., Sobel et al. 2010). While the maximum seasonal-mean convection is found at the island (Fig. 1a), the maximum variance is observed over the ocean around 5°S (Fig. 1d). This may suggest that the detailed processes that determine seasonal-mean convection and subseasonal convective variability are somewhat different.

As in seasonal-mean convection, the subseasonal convective activity varies significantly from year to year (e.g., Hendon et al. 1999). Figure 1e presents the ENSO-related OLR variance change in DJF. A significant change appears around the date line, with an enhanced variance during El Niño winters. This change is consistent with an eastward extension of mean convection during El Niño winters as depicted in Fig. 1b. However, across the Maritime Continent, the ENSO-related OLR variance change is almost negligible. This result indicates that although subseasonal convective activity, including the MJO, tends to extend farther eastward during El Niño winters (Gualdi et al. 1999; Hendon et al. 1999, 2007; Gushchina and Bewitte 2012), its intensity around the Maritime Continent is not strongly regulated by the ENSO. The same result is also found in other seasons (Table 1).

It should be noted that the above result, which is based on linear correlation and composite analyses, does not necessarily indicate that ENSO has no impacts on MJO amplitude. In fact, recent studies reported a significant ENSO–MJO link during boreal winter (Feng et al. 2015; Pang et al. 2016). Such a relationship, however, is nonlinear and highly dependent on the characteristics of ENSO itself. For example, it is shown that the MJO becomes stronger than normal during the central Pacific El Niño winters whereas it becomes weaker during the eastern Pacific El Niño winters (Feng et al. 2015; Pang et al. 2016). The sum of these contrasting responses likely results in no systematic changes in MJO amplitude during all El Niño winters. As such, the above result, summarized in Fig. 1 and Table 1, should be taken as a first-order linear relationship.

Apart from nonlinear impacts of the ENSO, what determines the interannual variation of MJO-related subseasonal convective activity? Figure 1f suggests that it is likely the QBO. Near-equatorial OLR variances, across the central Indian Ocean and western Pacific, are typically stronger during EQBO winters (i.e., when DJF U50 is easterly) than WQBO winters. Their differences reach up to 40%–50% of the climatological OLR variance around the Maritime Continent (cf. Figs. 1d,f). More importantly, unlike the ENSO-related OLR variance change (Fig. 1e), the QBO-related change is centered at 5°S and almost exclusively present in the Indo-Pacific region, from 60°E to 180°, where MJO is active during boreal winter [see also Yoo and Son (2016)].

The ENSO–MJO and QBO–MJO relationships are further evaluated by correlation analyses. Linear correlations are computed for the DJF-mean MJO amplitude against various ENSO and QBO indices (see the MJO column in Table 1). No significant link is found between ENSO and MJO amplitude in all seasons, supporting previous studies (e.g., Hendon et al. 1999, 2007). In contrast, during boreal winter, statistically significant correlations with the QBO, which are greater than ±0.5, are observed from the upper stratosphere (i.e., 10 hPa) to the lower stratosphere (i.e., 50 hPa) with a switching sign. This height-dependent correlation represents a quasi-periodic downward propagation of zonal-mean zonal wind in association with the QBO (see also Fig. 6b, which is discussed later). Note that the correlation coefficient for the zonal-mean zonal wind at 10 hPa (U10) is larger than the one at 50 hPa (U50). This is partly due to the internal variability of zonal-mean zonal wind in the lower stratosphere, which is introduced by the wave activities in the upper troposphere and lower stratosphere. When high-frequency variability is filtered out, the 50-hPa correlation becomes comparable to the 10-hPa correlation (not shown). Note also that the QBO–MJO link appears only in the boreal winter (Table 1). This seasonality is discussed later.

a. QBO–MJO link

To establish the QBO–MJO link more directly, composite OLR anomalies are presented for each MJO phase (Fig. 2). In Fig. 2, the number of samples used in composite map is denoted at the top-left corner of each panel, and the values that are statistically significant at the 95% confidence level are contoured. Here, a

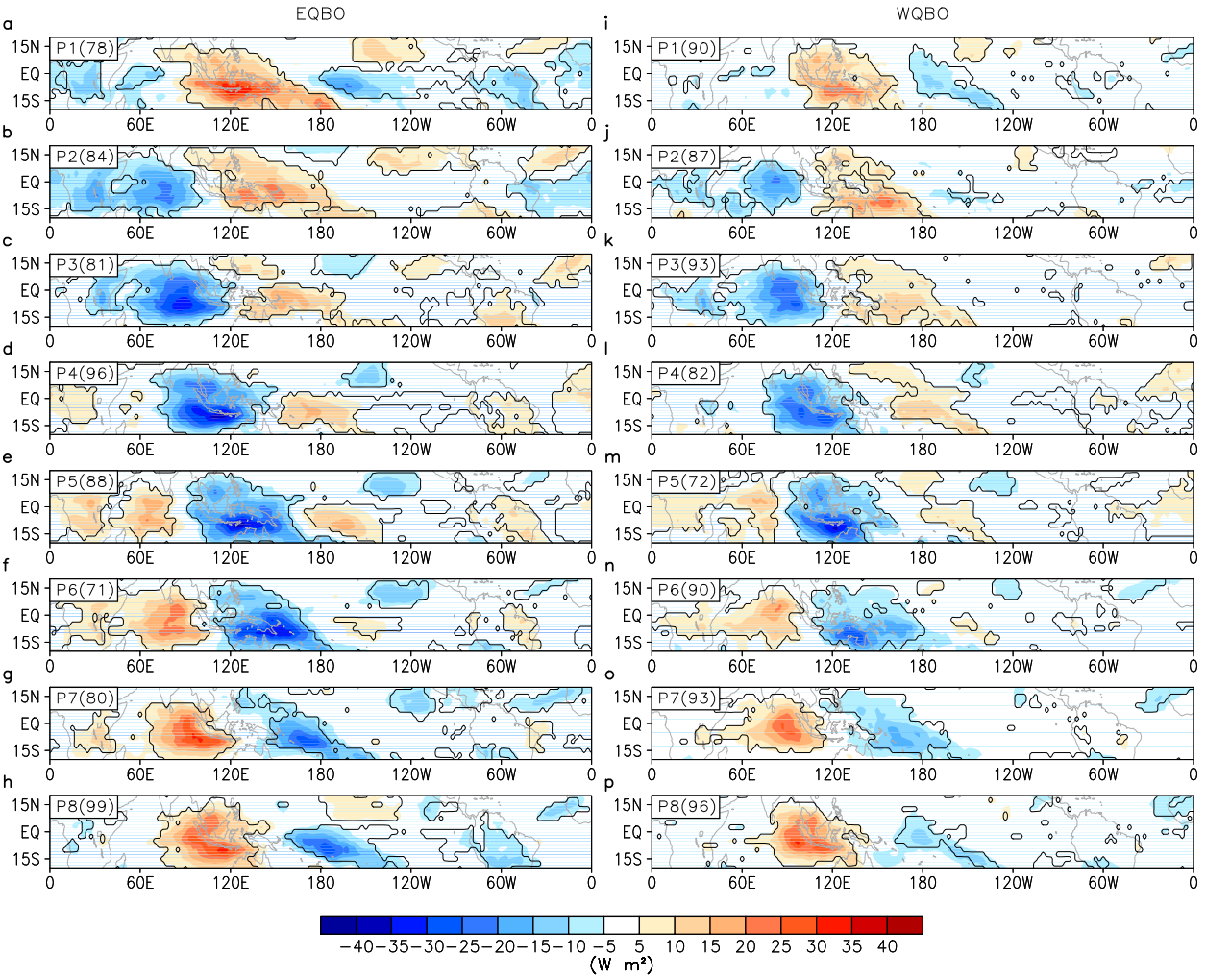

FIG. 2. Composite of bandpass-filtered (20–100 days) OLR anomaly for each MJO phase during (a)–(h) EQBO and (i)–(p) WQBO winters. Only days when the MJO amplitude is greater than 1.0 are used, and seasonal-mean values in each year are subtracted to remove interannual variation of background flow. Sample size is denoted at the top-left corner of each panel in parentheses, and statistically significant values at the 95% confidence level are contoured.

statistical significance test is performed using a Student's t test by counting the number of degrees of freedom only when each day in a given phase is separated by at least seven days (Garfinkel et al. 2012). It is evident from Fig. 2 that, for most MJO phases, the OLR anomalies, subject to bandpass filtering (20–100 days), are stronger during EQBO winters than WQBO winters. If only active MJOs are considered (i.e., when the MJO amplitude exceeds 1 and consistently propagates eastward in time), their differences become even larger and statistically significant for all MJO phases (Yoo and Son 2016). Although not shown, this result is not sensitive to the inclusion or exclusion of strong ENSO years.

Although OLR is widely used to quantify tropical deep convection, it does not necessarily represent precipitating clouds. In other words, the QBO–MJO relationship, illustrated in Fig. 2, may simply represent nonprecipitating cloud changes in the upper troposphere. To test such a possibility, the same analysis is repeated with high-resolution precipitation data (Fig. 3). The same result, with a much larger difference between EQBO and WQBO winters, is obtained. This result clearly indicates that, on interannual time scales, the MJO-related subseasonal convective activity is more sensitive to the stratospheric mean state change than the SST change associated with ENSO.

The QBO–MJO link is evident not only in the MJO amplitude but also in the propagation speed and frequency of MJO. Although not shown, the power spectrum of planetary-scale OLR anomalies, averaged over 15°S–5°N, becomes broader during EQBO

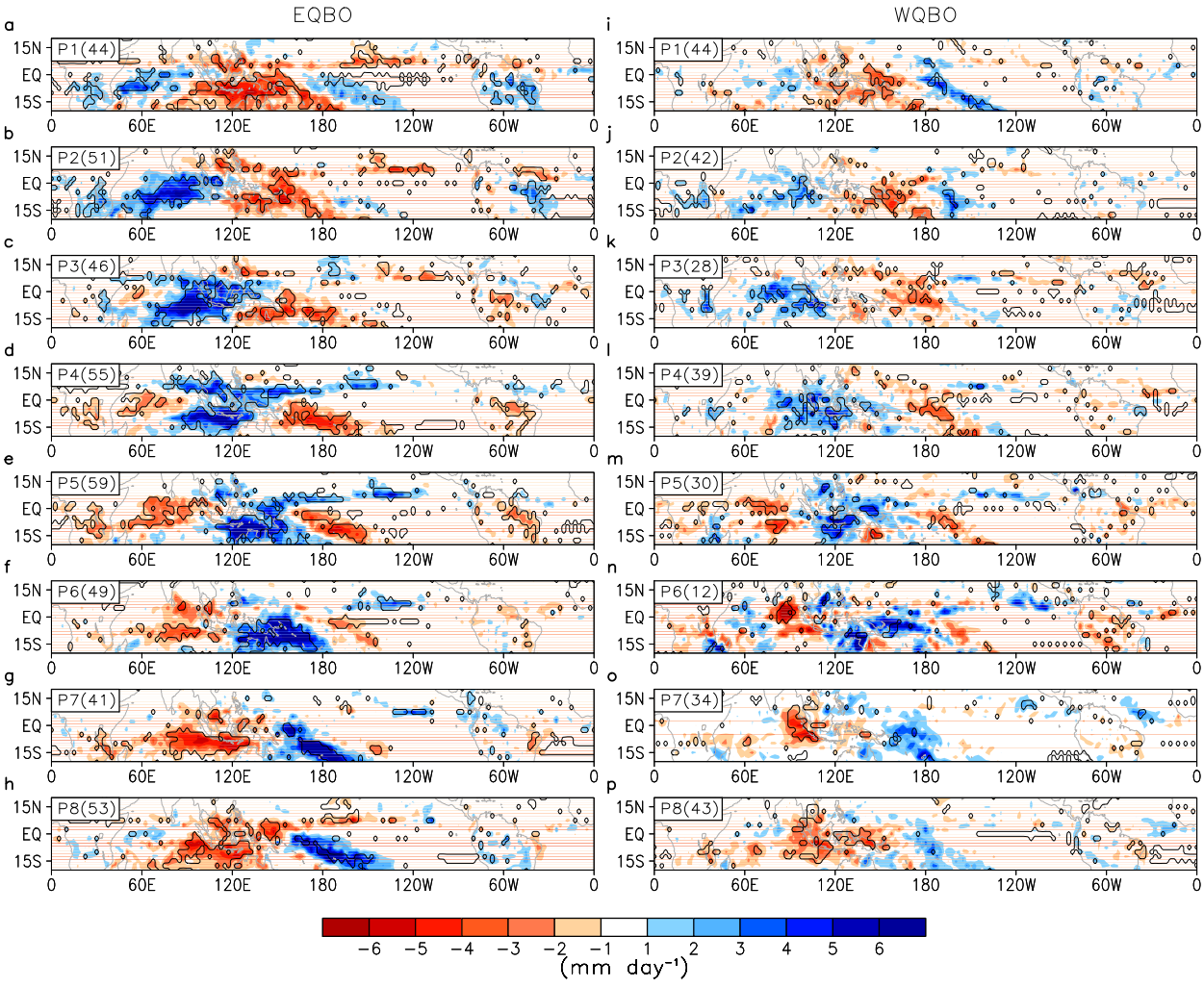

FIG. 3. As in Fig. 2, but for TRMM precipitation.

winters, with a reduced quasi-stationary variability. Consistent with this spectrum change, eastward propagation of OLR anomalies and the associated lower-tropospheric circulations become more pronounced during EQBO winters (Fig. 4). Their propagation speed is also somewhat slower (see also Nishimoto and Yoden 2017). Most importantly, the period of MJO, estimated by the distance from the center of blue shading at negative lags to that at positive lags in Fig. 4, becomes longer during EQBO winters. Based on auto-lag correlation of PC1, it is found that the MJO period during EQBO winters is about 50 days. This is about 10 days longer than the estimated MJO period during WQBO winters.

A slower propagation and longer period of MJO during EQBO winters may be simply explained by the MJO amplitude change itself. A simple composite analysis has shown that strong MJO events, regardless of the QBO, tend to propagate more slowly across the Maritime Continent than weak MJO events (Seo and Kumar 2008). They also exhibit a longer period than the latter (Seo and Kumar 2008). Although the MJO propagation is not simply controlled by the equatorial waves, it is at least in part influenced by the phase speed of planetary-scale Kelvin waves. In a simple model, the Kelvin waves become slower when diabatic heating (or precipitation rate) increases [e.g., Chang (1977) or, more recently, Kang et al. (2013)]. This may imply a slower MJO propagation when the MJO-related convection becomes stronger. If a new MJO over the Indian Ocean is initiated by the decaying MJO over the western Pacific (e.g., Zhao et al. 2013), a slower MJO propagation to the Pacific would then result in a delayed MJO initiation. This may lead to a longer period of MJO events. Based on these speculations, we argue that a key

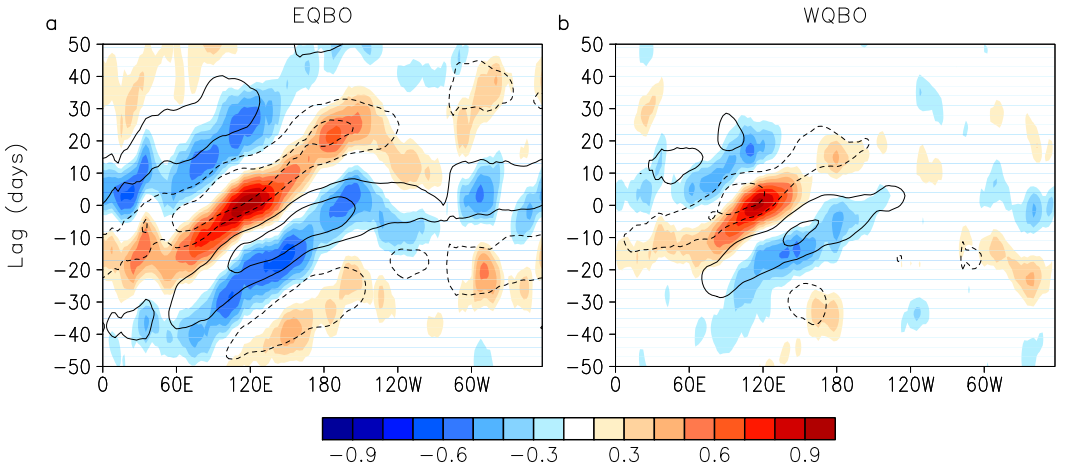

FIG. 4. Correlation coefficient of OLR (shading) and 850-hPa zonal wind anomalies (contour), averaged over 15°S–5°N, against OLR anomaly around the Maritime Continent (15°S–5°N, 100°–130°E) during boreal winter. The shading and contour intervals are 0.3 and 0.1, respectively. Zero contours are omitted.

factor of the QBO–MJO link is the QBO-related MJO amplitude change.

A stronger and more organized MJO during EQBO winters also implies an enhanced MJO-related tropical–extratropical teleconnection. This is indeed the case. Figure 5 presents the time-lagged composite of 300-hPa streamfunction anomalies for the MJO phases 2 and 3 when the MJO convection is located over the Indian Ocean. The MJO teleconnections [i.e., strong positive anomaly over South Asia and a wave train across the North Pacific (e.g., Lin et al. 2009)] is more pronounced during EQBO winters (Figs. 5a,b). In contrast, the overall pattern is less organized during WQBO winters especially at lag 10 days (Figs. 5c,d). Here it should be emphasized that the enhanced MJO teleconnections appear to be primarily driven by the strengthened convection itself. This contrasts with the ENSO modulation of the MJO teleconnections that is associated with background flow change (Moon et al. 2011). Although the QBO also accompanies a subtropical jet change (Baldwin et al. 2001; Garfinkel and Hartmann 2010), such a change is much weaker than the one for the ENSO and does not likely affect the MJO teleconnections. More details of QBO-induced MJO teleconnection changes will be documented in a future study.

b. *Lead–lag relationship of the QBO–MJO link*

The above results do not necessarily reveal a causal relationship as time lags are not taken into account. That is, the QBO–MJO link may not result from the downward influence of the QBO. It could be instead caused by the upward influence of the MJO. In fact, it is well established that the QBO is influenced by the convectively coupled gravity waves (Baldwin et al. 2001) and is better simulated when a parameterization of convectively driven gravity waves is implemented in the model (Kim et al. 2013).

Figure 6a shows the lead–lag correlation of 3-month running-mean U50 against the DJF MJO amplitude. Negative lags indicate that the former leads the latter. Statistically significant correlations are observed from lag −6 (June–August) to lag 2 months (February–April). Although it is not distinguishable by eyes, the maximum negative correlation is found at lag −2, that is, U50 leading DJF MJO amplitude about two months [see also Marshall et al. (2016)]. To better understand this lead–lag relationship, the analysis is extended to the whole stratosphere (Fig. 6b). Unlike at 50 hPa, maximum correlation at 10 hPa appears at positive lags, possibly indicating a modulation of QBO by the MJO. However, even at 10 hPa, significant correlations start to appear at negative time lags. More importantly, they propagate downward in time, reflecting a quasi-periodic oscillation of the QBO, with a much longer time scale than the time scale of MJO itself. This result suggests that the QBO–MJO link is mostly downward from the stratosphere to the troposphere although the upward influence is not negligible. A possible two-way interaction between the QBO and MJO deserves further analysis.

c. *Seasonality of the QBO–MJO link*

As highlighted in Yoo and Son (2016), the QBO–MJO link appears only in the boreal winter (see Table 1). No significant relationships are found in other seasons. Even in spring when MJO is still active, the QBO–MJO link is almost absent. This seasonal dependency may partly result from the seasonality of the QBO phase

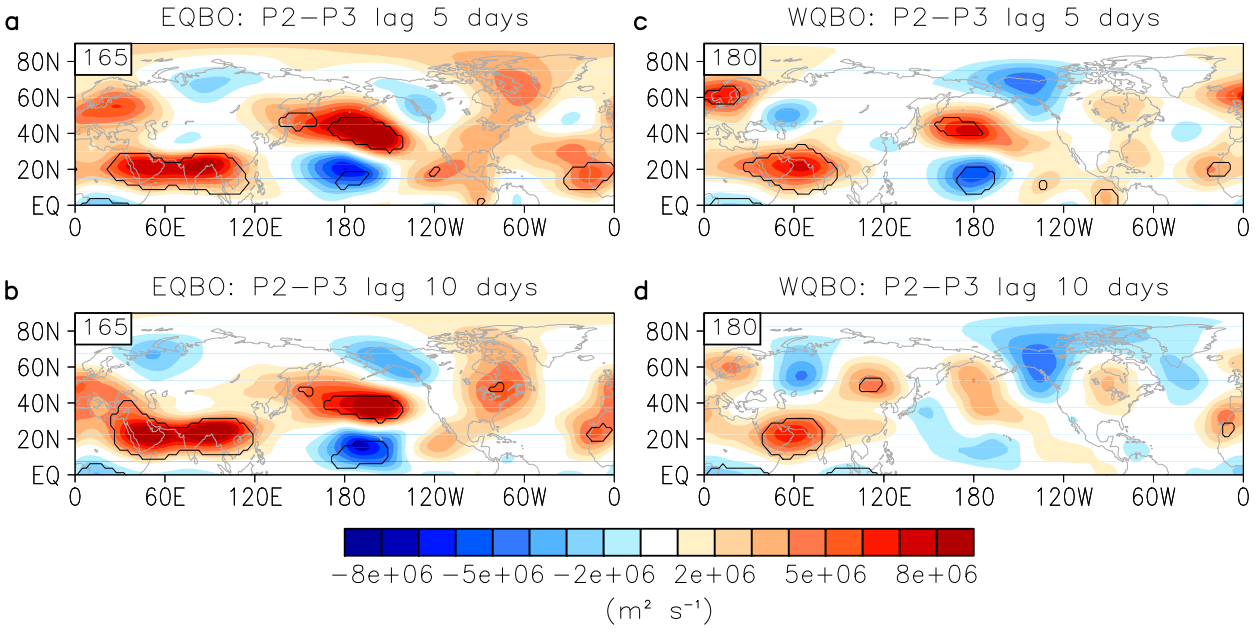

FIG. 5. Lagged composite of 300-hPa streamfunction anomaly for MJO phases 2 and 3 when organized convective activity is located at the eastern Indian Ocean. (a),(c) Lag 5 and (b),(d) lag 10 days are shown for (a),(b) EQBO and (c),(d) WQBO winter, separately. Only days when the MJO amplitude is greater than 1.0 are used, and the seasonal-mean values in each year are subtracted to remove the interannual variation of background flow. To reduce noise, a 5-day running mean average is also applied. Statistically significant values at the 95% confidence level are contoured.

transition. The QBO tends to change its phase approximately every 14 months. During the analysis period (1979–2013), it primarily occurred in spring with a minimum variance of U50 (not shown). In other words, the QBO-related mean state is relatively weak in spring compared to other seasons, possibly explaining a rather weak influence of the QBO on springtime MJO. Other possible factor is a seasonal cycle of tropopause. The tropical tropopause is highest during boreal winter (Kim and Son 2012). This observation suggests that the QBO changes tropopause properties most effectively during boreal winter. If the MJO is influenced by the dynamical and physical processes near the tropopause as discussed below, this suggests more effective modulation of the MJO by the QBO during boreal winter than during boreal spring.

During summer and fall, the MJO itself is weak and not well organized (Zhang 2013). In particular, the summertime MJO tends to propagate northward, away from the equator where the QBO is active. These conditions may explain a negligible QBO–MJO connection in these seasons (Yoo and Son 2016). To confirm these speculations, further studies are needed.

d. Possible mechanism(s) of the QBO–MJO link

It is unclear how the QBO affects the MJO. One of the possible mechanisms is the static stability change in the upper troposphere (Reid and Gage 1985; Gray et al. 1992; Giorgetta et al. 1999; Garfinkel and Hartmann 2011; Yoo and Son 2016). The downward propagation of zonal-mean zonal wind accompanies the secondary circulation in the subtropical stratosphere as a result of the thermal wind balance (Baldwin et al. 2001). The net result is a vertical pair of adiabatic cooling and warming at the equatorial stratosphere (Figs. 7a,b). Although less organized, a hint of adiabatic warming and cooling also appears in the Northern Hemisphere subtropics, reflecting returning flow of the secondary circulation. The zonal wind and temperature anomalies also appear in the polar stratosphere (Figs. 7a,b). This is caused by planetary-scale wave and zonal mean flow interaction in the extratropical stratosphere (Holton and Tan 1980) and not directly relevant to the QBO–MJO link.

The observed zonal wind and temperature profiles are further illustrated in Figs. 7c and 7d from long-term radiosonde observations. In spite of large interannual variability, QBO-related temperature anomalies that are greater than ±1 K are evident in the lower stratosphere. More importantly, these temperature anomalies, centered at 70 hPa, are not confined within the stratosphere but extend to the upper troposphere below 100 hPa (Note that the DJF-mean tropopause in this region is located at ~100 hPa). The static stability

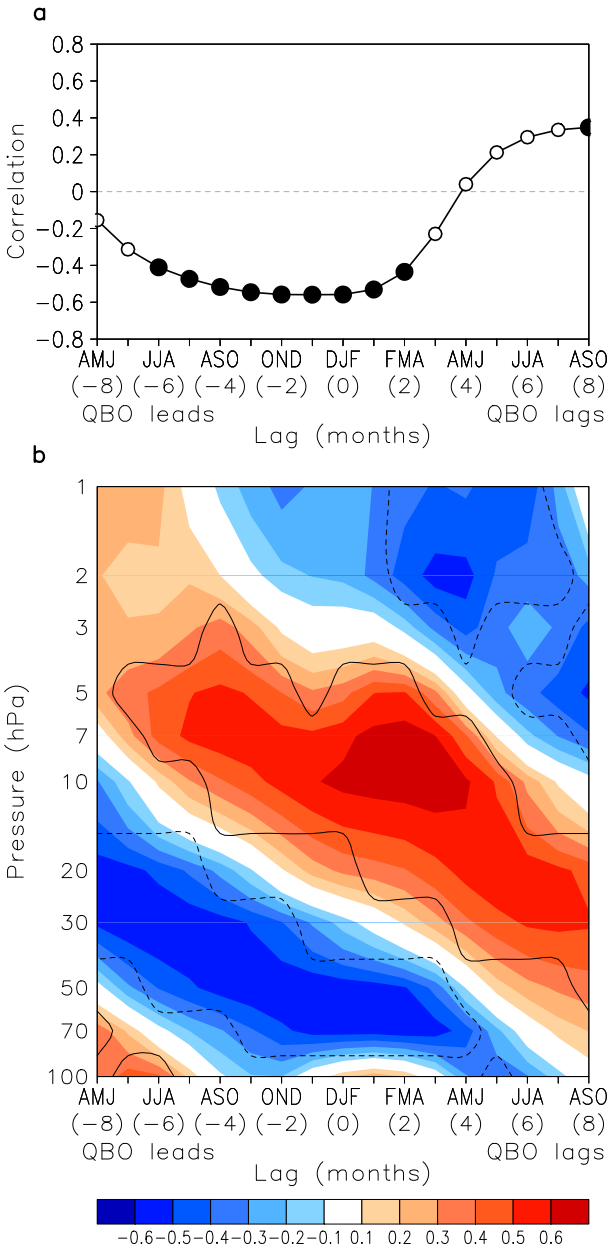

FIG. 6. (a) Lead–lag correlation of U50 against the DJF MJO amplitude and (b) its extension to the whole stratosphere. Statistically significant values at the 95% confidence level are denoted with filled circles in (a) and are contoured in (b). Positive lag indicates that the DJF MJO amplitude leads QBO.

changes, which are proportional to the vertical gradient of temperature profiles, are observed even at 150 hPa (Fig. 7e). A qualitatively similar result is also found in the high-resolution temperature profiles derived from the COSMIC GPS RO measurements (not shown).

Figure 7e indicates that the near-tropopause static stability is relatively weaker during EQBO winters. If the MJO, which is well organized in the vertical, is influenced by the static stability near the tropical tropopause, such a destabilization could enhance the MJO. This possibility is supported by the recent modeling study (Nie and Sobel 2015). On the other hand, since the QBO may regulate only organized high-top clouds (Collimore et al. 2003), its influence on seasonal-mean convection, which consists of various clouds such as low-, mid-, and high-top clouds, would be rather minor (Fig. 1c).

The near-tropopause static stability change, caused by adiabatic heating associated with the QBO-induced secondary circulation, may be further enhanced by the diabatic process resulting from cirrus clouds. As shown in Fig. 7d, tropopause temperature is much colder during EQBO winters than WQBO winters. This may allow more frequent formation of cirrus clouds near the tropopause. Figures 8a and 8b illustrate the spatial distribution of the DJF-mean temperature at the cold-point tropopause as derived from COSMIC GPS RO measurements. Because the longitudinal distribution of the tropical tropopause temperature is largely determined by the underlying convection (Kim and Son 2012), its spatial pattern follows the DJF-mean OLR distribution very well (cf. Fig. 1a and Figs. 8a,b). However, the QBO-related tropopause temperature change, up to −2 K, is largely homogeneous in the deep tropics.

Figures 8d–f show that the fraction of cirrus clouds, estimated from CALIOP measurements, is sensitive to the tropopause temperature. For colder tropopause temperature during EQBO winter, cirrus clouds form more frequently especially across the Maritime Continent and central Pacific (Fig. 8f). Because near-tropopause cirrus clouds result in a net radiative cooling in the lower stratosphere and warming in the troposphere (Hartmann et al. 2001; Yang et al. 2010; Hong et al. 2016), this may destabilize the tropical upper troposphere, especially near the tropopause, helping a development of the organized deep convection. Note that even without cirrus clouds, the cold tropopause itself could provide a favorable environment for organized deep convection (e.g., Emanuel et al. 2013).

The adiabatic and diabatic processes described above may not be the sole potential mechanism that affects the MJO. Other mechanisms, which may include vertical wind shear (Gray et al. 1992; Collimore et al. 2003; Ho et al. 2009), absolute vorticity (Collimore et al. 2003), and tropopause changes (Reid and Gage 1985; Gray et al. 1992), are not exclusive. Presumably, the QBO–MJO link is associated with multiple factors. To identify the exact mechanism(s),

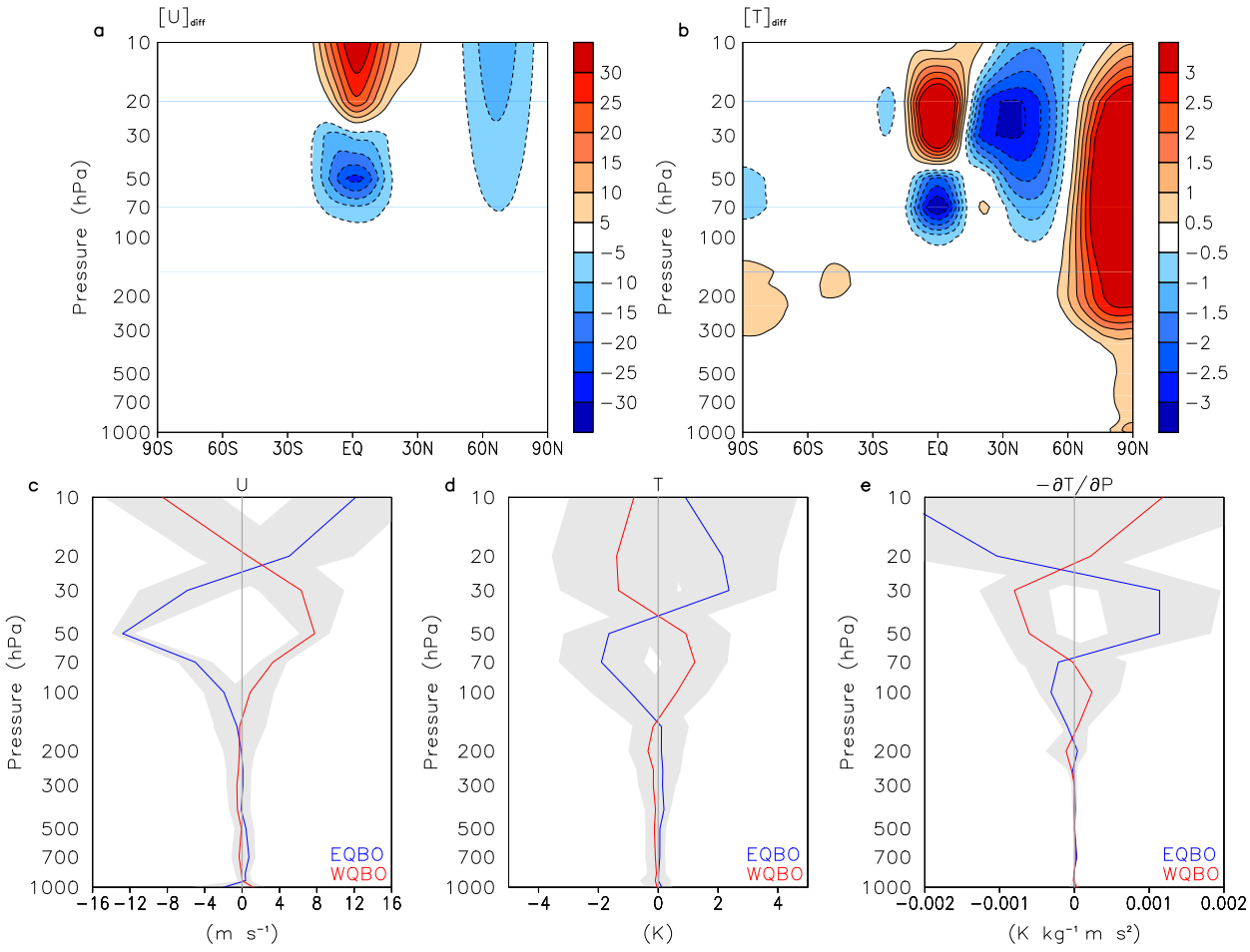

FIG. 7. Difference in zonal-mean (a) zonal wind ($m\,s^{-1}$) and (b) temperature (K) between EQBO and WQBO winters from the ERA-Interim. (c) Observed zonal wind, (d) temperature, and (e) vertical temperature gradient anomalies averaged over six IGRA stations around the Maritime Continent, during EQBO (blue) and WQBO (red) winters. The 0.5 standard deviation range is shown in gray.

further studies, using both observations and numerical models, are needed. In this regard, a cloud-resolving model experiment (e.g., Nie and Sobel 2015) would be very useful.

5. Summary

This study examines the relative importance of ENSO and QBO on the interannual variation of large-scale tropical convection. Both seasonal-mean and subseasonal variability are analyzed. It is found that the interannual variation of seasonal-mean convection, especially that over the equatorial Pacific, is primarily controlled by the ENSO with a minor contribution of the QBO. In terms of linear correlation, the ENSO explains about 50%–70% of interannual variation of the DJF-mean OLR across the Maritime Continent and western tropical Pacific (Table 1).

The ENSO also affects the spatial distribution of subseasonal convective activity such as MJO. The MJO activity tends to extend farther into the central Pacific during El Niño winters and the opposite during La Niña winters. However, ENSO does not systematically change overall amplitude of the MJO. The MJO amplitude is instead highly modulated by the QBO. In terms of linear correlation, the QBO explains about 30%–40% of interannual variation of the DJF MJO amplitude. Such a link between QBO and MJO is also found in other MJO properties (i.e., a stronger amplitude, slower propagation, and longer period of MJO during EQBO winters). The MJO-induced teleconnections are also more pronounced during EQBO winters. Although the dynamic and physical mechanism(s) are unclear, this QBO–MJO link is consistent with the thermal stratification change in the upper troposphere. However, other processes such as

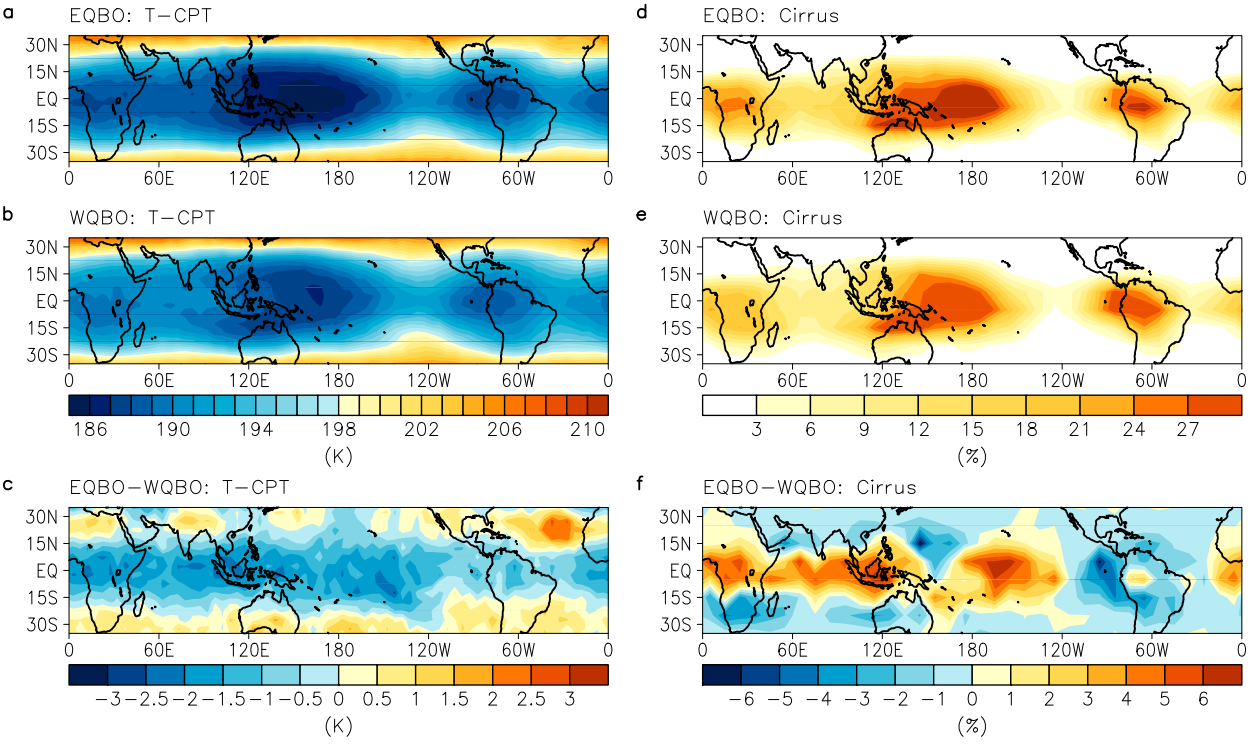

FIG. 8. Spatial distribution of DJF-mean temperature at the cold-point tropopause (K), derived from the COSMIC GPS RO measurements, for (a) EQBO and (b) WQBO winters and (c) their difference. (d)–(f) As in (a)–(c), but for the near-tropopause cirrus frequency (%) from the CALIOP measurements.

inertial instability, moist processes, and radiative feedback changes may also be important. To identify the exact mechanism(s), further studies using both observations and numerical model simulations are necessary.

Our findings suggest that to better understand and predict the MJO, not only the tropospheric circulation but also the stratospheric circulation should be taken into account. It is further suggested that subseasonal-to-seasonal prediction of the MJO and the related teleconnections may be sensitive to the stratospheric mean state. A preliminary result indeed showed that the MJO is better predicted during EQBO winters than WQBO winters (Marshall et al. 2016). Given the fact that the QBO is highly predictable (e.g., Scaife et al. 2014), this result also opens a new avenue of seasonal-to-interannual prediction of the MJO.

Acknowledgments. We thank the ECMWF, NOAA, UCAR, and NASA for providing us with the reanalysis data and various satellite datasets. We also thank Sang-Woo Kim for processing CALIOP data, and Daehyun Kim, Fei Liu, and Kyong-Hwan Seo for helpful discussion. This work is supported by the Korea Meteorological Administration Research and Development Program under Grant KMIPA 2015-2094 and by the National Research Foundation of Korea under Grant NRF-2016R1C1B2006310.

REFERENCES

Anthes, R. A., and Coauthors, 2008: The COSMIC/FORMOSAT-3 mission: Early results. *Bull. Amer. Meteor. Soc.*, **89**, 313–333, doi:10.1175/BAMS-89-3-313.

Baldwin, M. P., and Coauthors, 2001: The quasi-biennial oscillation. *Rev. Geophys.*, **39**, 179–229, doi:10.1029/1999RG000073.

Chang, C.-P., 1977: Viscous internal gravity waves and low-frequency oscillations in the tropics. *J. Atmos. Sci.*, **34**, 901–910, doi:10.1175/1520-0469(1977)034<0901:VIGWAL>2.0.CO;2.

Collimore, C. C., D. W. Martin, M. H. Hitchman, A. Huesmann, and D. E. Waliser, 2003: On the relationship between the QBO and tropical deep convection. *J. Climate*, **16**, 2552–2568, doi:10.1175/1520-0442(2003)016<2552:OTRBTQ>2.0.CO;2.

Dee, D. P., and Coauthors, 2011: The ERA-Interim reanalysis: Configuration and performance of the data assimilation system. *Quart. J. Roy. Meteor. Soc.*, **137**, 553–597, doi:10.1002/qj.828.

Durre, I., R. S. Vose, and D. B. Wuertz, 2006: Overview of the Integrated Global Radiosonde Archive. *J. Climate*, **19**, 53–68, doi:10.1175/JCLI3594.1.

Emanuel, K., S. Solomon, D. Folini, S. Davis, and C. Cagnazzo, 2013: Influence of tropical tropopause layer cooling on Atlantic hurricane activity. *J. Climate*, **26**, 2288–2301, doi:10.1175/JCLI-D-12-00242.1.

Feng, J., P. Liu, W. Chen, and X. Wang, 2015: Contrasting Madden–Julian oscillation activity during various stages of EP and CP El Niños. *Atmos. Sci. Lett.*, **16**, 32–37, doi:10.1002/asl2.516.

Garfinkel, C. I., and D. L. Hartmann, 2010: Influence of the quasi-biennial oscillation on the North Pacific and El Niño teleconnections. *J. Geophys. Res.*, **115**, D20116, doi:10.1029/2010JD014181.

——, and ——, 2011: The influence of the quasi-biennial oscillation on the troposphere in wintertime in a hierarchy of models. Part II: Perpetual winter WACCM runs. *J. Atmos. Sci.*, **68**, 2026–2041, doi:10.1175/2011JAS3702.1.

——, S. B. Feldstein, D. W. Waugh, C. Yoo, and S. Lee, 2012: Observed connection between stratospheric sudden warmings and the Madden–Julian oscillation. *Geophys. Res. Lett.*, **39**, L18807, doi:10.1029/2012GL053144.

Giorgetta, M. A., L. Bengtsson, and K. Arpe, 1999: An investigation of QBO signals in the East Asian and Indian monsoon in GCM experiments. *Climate Dyn.*, **15**, 435–450, doi:10.1007/s003820050292.

Gray, W. M., J. D. Sheaffer, and J. A. Knaff, 1992: Hypothesized mechanism for stratospheric QBO influence on ENSO variability. *Geophys. Res. Lett.*, **19**, 107–110, doi:10.1029/91GL02950.

Gualdi, S., A. Navarra, and G. Tinarelli, 1999: The interannual variability of the Madden–Julian oscillation in an ensemble of GCM simulations. *Climate Dyn.*, **15**, 643–658, doi:10.1007/s003820050307.

Gushchina, D., and B. Dewitte, 2012: Intraseasonal tropical atmospheric variability associated with the two flavors of El Niño. *Mon. Wea. Rev.*, **140**, 3669–3681, doi:10.1175/MWR-D-11-00267.1.

Hartmann, D. L., J. R. Holton, and Q. Fu, 2001: The heat balance of the tropical tropopause, cirrus, and stratospheric dehydration. *Geophys. Res. Lett.*, **28**, 1969–1972, doi:10.1029/2000GL012833.

Hendon, H. H., C. Zhang, and J. D. Glick, 1999: Interannual variation of the Madden–Julian oscillation during austral summer. *J. Climate*, **12**, 2538–2550, doi:10.1175/1520-0442(1999)012<2538:IVOTMJ>2.0.CO;2.

——, M. C. Wheeler, and C. Zhang, 2007: Seasonal dependence of the MJO–ENSO relationship. *J. Climate*, **20**, 531–543, doi:10.1175/JCLI4003.1.

Ho, C.-H., H.-S. Kim, J.-H. Jeong, and S.-W. Son, 2009: Influence of stratospheric quasi-biennial oscillation on tropical cyclone tracks in western North Pacific. *Geophys. Res. Lett.*, **36**, L06702, doi:10.1029/2009GL037163.

Holton, J. R., and H. C. Tan, 1980: The influence of the equatorial quasi-biennial oscillation on the global circulation at 50 mb. *J. Atmos. Sci.*, **37**, 2200–2208, doi:10.1175/1520-0469(1980)037<2200:TIOTEQ>2.0.CO;2.

Hong, Y., G. Liu, and J.-L. F. Li, 2016: Assessing the radiative effects of global ice clouds based on *CloudSat* and *CALIPSO* measurements. *J. Climate*, **29**, 7651–7674, doi:10.1175/JCLI-D-15-0799.1.

Huang, B., and Coauthors, 2016: Further exploring and quantifying uncertainties for Extended Reconstructed Sea Surface Temperature (ERSST) version 4 (v4). *J. Climate*, **29**, 3119–3142, doi:10.1175/JCLI-D-15-0430.1.

Inoue, M., M. Takahashi, and H. Naoe, 2011: Relationship between the stratospheric quasi-biennial oscillation and tropospheric circulation in northern autumn. *J. Geophys. Res.*, **116**, D24115, doi:10.1029/2011JD016040.

Jin, F., and B. J. Hoskins, 1995: The direct response to tropical heating in a baroclinic atmosphere. *J. Atmos. Sci.*, **52**, 307–319, doi:10.1175/1520-0469(1995)052<0307:TDRTTH>2.0.CO;2.

Kang, I.-S., F. Liu, M.-S. Ahn, Y.-M. Yang, and B. Wang, 2013: The role of SST structure in convectively coupled Kelvin–Rossby waves and its implication for MJO formation. *J. Climate*, **26**, 5915–5930, doi:10.1175/JCLI-D-12-00303.1.

Kiladis, G. N., and Coauthors, 2014: A comparison of OLR and circulation-based indices for tracking the MJO. *Mon. Wea. Rev.*, **142**, 1697–1715, doi:10.1175/MWR-D-13-00301.1.

Kim, J., and S.-W. Son, 2012: Tropical cold-point tropopause: Climatology, seasonal cycle, and intraseasonal variability derived from COSMIC GPS radio occultation measurements. *J. Climate*, **25**, 5343–5360, doi:10.1175/JCLI-D-11-00554.1.

Kim, Y.-H., A. C. Bushell, D. R. Jackson, and H.-Y. Chun, 2013: Impacts of introducing a convective gravity-wave parameterization upon the QBO in the Met Office Unified Model. *Geophys. Res. Lett.*, **40**, 1873–1877, doi:10.1002/grl.50353.

Liebmann, B., and C. A. Smith, 1996: Description of a complete (interpolated) outgoing long-wave radiation dataset. *Bull. Amer. Meteor. Soc.*, **77**, 1275–1277.

Liess, S., and M. A. Geller, 2012: On the relationship between QBO and distribution of tropical deep convection. *J. Geophys. Res.*, **117**, D03108, doi:10.1029/2011JD016317.

Lin, H., G. Brunet, and J. Derome, 2009: An observed connection between the North Atlantic Oscillation and the Madden–Julian oscillation. *J. Climate*, **22**, 364–380, doi:10.1175/2008JCLI2515.1.

Liu, C., B. Tian, K.-F. Li, G. L. Manney, N. J. Livesey, Y. L. Yung, and D. E. Waliser, 2014: Northern Hemisphere mid-winter vortex-displacement and vortex-split stratospheric sudden warmings: Influence of the Madden–Julian oscillation and quasi-biennial oscillation. *J. Geophys. Res.*, **119**, 12 599–12 620, doi:10.1002/2014JD021876.

Liu, Z., D. Ostrenga, W. Teng, and S. Kempler, 2012: Tropical Rainfall Measuring Mission (TRMM) precipitation data and services for research and applications. *Bull. Amer. Meteor. Soc.*, **93**, 1317–1325, doi:10.1175/BAMS-D-11-00152.1.

Madden, R., and P. Julian, 1994: Observations of the 40–50-day tropical oscillation—A review. *Mon. Wea. Rev.*, **122**, 814–837, doi:10.1175/1520-0493(1994)122<0814:OOTDTO>2.0.CO;2.

Marshall, A. G., H. H. Hendon, S.-W. Son, and Y. Lim, 2016: Impact of the quasi-biennial oscillation on predictability of the Madden–Julian oscillation. *Climate Dyn.,* doi:10.1007/s00382-016-3392-0, in press.

Martin, D. W., C. C. Collimore, and M. H. Hitchman, 2004: El Niño and La Niña in highly reflective cloud. *J. Climate*, **17**, 3470–3475, doi:10.1175/1520-0442(2004)017<3470:ENALNI>2.0.CO;2.

Moon, J.-Y., B. Wang, and K.-J. Ha, 2011: ENSO regulation of MJO teleconnection. *Climate Dyn.*, **37**, 1133–1149, doi:10.1007/s00382-010-0902-3.

Naujokat, B., 1986: An update of the observed quasi-biennial oscillation of the stratospheric winds over the tropics. *J. Atmos. Sci.*, **43**, 1873–1877, doi:10.1175/1520-0469(1986)043<1873:AUOTOQ>2.0.CO;2.

Nie, J., and A. H. Sobel, 2015: Responses of tropical deep convection to the QBO: Cloud-resolving simulations. *J. Atmos. Sci.*, **72**, 3625–3638, doi:10.1175/JAS-D-15-0035.1.

Nishimoto, E., and S. Yoden, 2017: Influence of the stratospheric quasi-biennial oscillation on the Madden–Julian oscillation during austral summer. *J. Atmos. Sci.*, doi:10.1175/JAS-D-16-0205.1, in press.

Pang, B., Z. Chen, Z. Wen, and R. Lu, 2016: Impacts of two types of El Niño on the MJO during boreal winter. *Adv. Atmos. Sci.*, **33**, 979–986, doi:10.1007/s00376-016-5272-2.

Reid, G. C., and K. S. Gage, 1985: Interannual variations in the height of the tropical tropopause. *J. Geophys. Res.*, **90**, 5629–5635, doi:10.1029/JD090iD03p05629.

Robertson, A. W., A. Kumar, M. Peña, and F. Vitart, 2015: Improving and promoting subseasonal to seasonal prediction. *Bull. Amer. Meteor. Soc.*, **96**, ES49–ES53, doi:10.1175/BAMS-D-14-00139.1.

Sassen, K., Z. Wang, and D. Liu, 2008: The global distribution of cirrus clouds from *CloudSat*/*Cloud–Aerosol Lidar and Infrared Pathfinder Satellite Observations* (*CALIPSO*) measurements. *J. Geophys. Res.*, **113**, D00A12, doi:10.1029/2008JD009972.

Scaife, A. A., and Coauthors, 2014: Predictability of the quasi-biennial oscillation and its northern winter teleconnection on seasonal to decadal timescales. *Geophys. Res. Lett.*, **41**, 1752–1758, doi:10.1002/2013GL059160.

Seo, K.-H., and A. Kumar, 2008: The onset and life span of the Madden–Julian oscillation. *Theor. Appl. Climatol.*, **94**, 13–24, doi:10.1007/s00704-007-0340-2.

——, and S.-W. Son, 2012: The global atmospheric circulation response to tropical diabatic heating associated with the Madden–Julian oscillation during northern winter. *J. Atmos. Sci.*, **69**, 79–96, doi:10.1175/2011JAS3686.1.

Sobel, A. H., E. D. Maloney, G. Bellon, and D. M. Frierson, 2010: Surface fluxes and tropical intraseasonal variability: A reassessment. *J. Adv. Model. Earth Syst.*, **2**, 2, doi:10.3894/JAMES.2010.2.2.

Son, S.-W., N. F. Tandon, and L. M. Polvani, 2011: The fine-scale structure of the global tropopause derived from COSMIC GPS radio occultation measurements. *J. Geophys. Res.*, **116**, D20113, doi:10.1029/2011JD016030.

Wallace, J. M., and D. S. Gutzler, 1981: Teleconnections in the geopotential height field during the Northern Hemisphere winter. *Mon. Wea. Rev.*, **109**, 784–812, doi:10.1175/1520-0493(1981)109<0784:TITGHF>2.0.CO;2.

Wheeler, M. C., and H. H. Hendon, 2004: An all-season real-time multivariate MJO index: Development of an index for monitoring and prediction. *Mon. Wea. Rev.*, **132**, 1917–1932, doi:10.1175/1520-0493(2004)132<1917:AARMMI>2.0.CO;2.

Winker, D. M., W. H. Hunt, and M. J. McGill, 2007: Initial performance assessment of CALIOP. *Geophys. Res. Lett.*, **34**, L19803, doi:10.1029/2007GL030135.

Yang, Q., Q. Fu, and Y. Hu, 2010: Radiative impacts of clouds in the tropical tropopause layer, *J. Geophys. Res.*, **115**, D00H12, doi:10.1029/2009JD012393.

Yoo, C., and S.-W. Son, 2016: Modulation of the boreal wintertime Madden–Julian oscillation by the stratospheric quasi-biennial oscillation. *Geophys. Res. Lett.*, **43**, 1392–1398, doi:10.1002/2016GL067762.

Zhang, C., 2013: Madden–Julian oscillation: Bridging weather and climate. *Bull. Amer. Meteor. Soc.*, **94**, 1849–1870, doi:10.1175/BAMS-D-12-00026.1.

Zhao, C., T. Li, and T. Zhou, 2013: Precursor signals and processes associated with MJO initiation over the tropical Indian Ocean. *J. Climate*, **26**, 291–307, doi:10.1175/JCLI-D-12-00113.1.